An Indirect Reference Vector-Based Model Predictive Control for a Three-Phase PMSM Motor

SHUANGXIA NIU [ID][1], **(Senior Member, IEEE), YIXIAO LUO** [ID][1], **(Student Member, IEEE),**
WEINONG FU [ID][1], **AND XIAODONG ZHANG** [ID][2], **(Student Member, IEEE)**

[1]Department of Electrical Engineering, The Hong Kong Polytechnic University, Hong Kong
[2]Shenzhen In Drive Amperex Company, Ltd., Shenzhen 518108, China

Corresponding author: Yixiao Luo (yxluowhu@hotmail.com)

ABSTRACT Almost all of the existing reference vector based finite control set-model predictive control (FCS-MPC) methods for electric machines adopt the deadbeat control principle to directly obtain the reference vector. This paper proposes a computationally efficient control approach for a three phase permanent magnet synchronous motor (PMSM) based on indirect reference vector without using the deadbeat control. Instead of calculating a virtual reference vector in the traditional manner using deadbeat control, the reference vector is innovatively determined through two two-level bang-bang comparators. To improve the performance of the machine, the sampling period is subdivided into two equal time intervals and total 20 synthesized voltage vectors are obtained. Nevertheless, there is no need to evaluate all the 20 vectors by excluding the inappropriate vectors in advance using the reference vector based method, thus reducing the computation time. Moreover, with this proposed method, the complicated calculation of reference vector is avoided. Simulation and experimental results are presented to prove the effectiveness of the proposed method.

INDEX TERMS Direct torque control, model predictive control, discrete space vector, PMSM motor.

I. INTRODUCTION

Finite control set-model predictive control (FCS-MPC) have been increasingly explored for the electric machine drives [1]–[3], power converters [4], [5] in recent years. It is well known that the FCS-MPC possesses the definite advantages of fast dynamic response, intuitive implementation and flexible inclusion of the nonlinearities [1]–[5].

Despite of all the advantages, the conventional FCS-MPC presents poor control performance if only one single vector is applied in each sampling period. To overcome this problem, a natural solution is to insert the zero vector to adjust the duty ratio of the prediction vector [6]–[11]. Generally, there are two manners to achieve this goal. One is directly calculating the duty ratio based on the torque constraint [6], [7]. Another is assigning discrete duty ratios to the selected voltage vector, i.e. 0, 0.2, 0.4, 0.6, 0.8, 1 [10], [11]. However, the calculation of the duty ratio is complicated, especially for an interior

The associate editor coordinating the review of this manuscript and approving it for publication was Ton Do [ID].

permanent magnet synchronous machine (IPMSM). In addition, the variation of machine parameters affects the accuracy of calculated duty ratio. Meanwhile, assigning discrete duty ratios highly increases the number of prediction vectors since there are usually 6 duty ratio values assigned to each vector.

Apart from duty ratio regulation, another alternative is to expand the number of the voltage vectors by subdividing the sampling period into several equal time intervals. This attempt has been widely investigated in both MPC method [12]–[14] and direct torque control (DTC) method [15], [16]. Unfortunately, all the vectors are enumerated in [12], which costs a large amount of time. In addition, the multiple vectors based MPC have been introduced in [17], [18], where the deadbeat control based on space vector modulation is employed to obtain the optimal vector and its duty ratio. This method can not only improve the control performance but also reduce the computation time by excluding the inappropriate voltage vectors in advance. However, the derivation of the reference vector using deadbeat control is complicated.

To reduce the computation time, a reference vector based MPC is introduced in [13], [14], but the derivation of the reference vector using deadbeat control is complex. A different solution to alleviate the computation time using the torque or flux constraint to exclude the useless vectors in advance is introduced in [19], [20]. However, only one vector is applied in [19], [20], which results in poor performance. Meanwhile, only one constraint, either torque or flux deviation is used in [19], [20], which aims at reducing the number of prediction vectors rather than determining the reference vector. Moreover, if DTC method based on space vector modulation is used, the multilevel hysteresis comparators are usually required to select the appropriate vector from the extended sets of vectors, where a complicated switching table is involved.

To summarize, a common practice to reduce the computation time in MPC is excluding the inappropriate vectors in advance. This can be achieved by calculating a reference vector or using the torque or flux constrained look-up table. Meanwhile, the reference vector can be determined by using either deadbeat current control [16] or deadbeat torque and flux control [15]. Nevertheless, the complicated derivation of the reference vector is undesired, and the parameter variation will affect the control performance. Moreover, the existing single constraint-based look-up table in [19], [20] can only reduce the number of prediction vectors to some extent but not able to reduce the number of prediction vectors sufficiently when the control period is subdivided into two or more intervals.

Therefore, this paper proposes a novel MPC method to reduce the computation time as well as improve the control performance. First, the control period is divided into two equal time intervals to enhance the steady-state performance. However, this attempt will increase the number of voltage vectors. To solve this problem, an indirect reference vector based MPC is proposed in this paper. The key is to select a reference vector from the six virtual vectors or real vectors first using the DTC theory instead of deriving a reference vector directly. Then, according to the position of the reference vector selected, the other vectors that locate in the same region will be selected as the prediction vectors. Subsequently, a cost function is defined to evaluate the selected prediction vectors and determine the optimal one. To prove the superiority of the proposed method, the conventional MPC method directly evaluating the six active vectors is also implemented as the benchmark method. The simulations and experimentations are conducted to verify the validity of the proposed method.

II. MODEL PREDICTIVE CONTROL OF THE THREE-PHASE PMSM MOTOR

A. DISCRETE MATHEMATICAL MODELLING

The schematic of the three-phase PMSM motor drive system is shown in Figure 1. Using the forward Euler approximation [19], the machine variables can be described in the
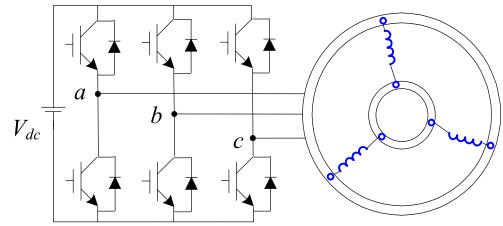

FIGURE 1. Three-phase two-level voltage source inverter fed PMSM motor.

discrete-time manner,

$$
\begin{cases}
\hat{i}_d(k+1) = (1 - \dfrac{R_s T_s}{L_d})i_d(k) + \dfrac{L_q}{L_d}\omega_r T_s i_q(k) + \dfrac{T_s}{L_d}v_d(k) \\
\hat{i}_q(k+1) = (1 - \dfrac{R_s T_s}{L_q})i_q(k) - \dfrac{L_d}{L_q}\omega_r T_s i_d(k) + \dfrac{T_s}{L_q}v_q(k)
\end{cases}
\tag{1}
$$

Accordingly, the flux at instant $k+1$ in the d-q axis can be expressed as

$$
\begin{cases}
\hat{\psi}_d(k+1) = \hat{i}_d(k+1)L_d + \psi_f \\
\hat{\psi}_q(k+1) = \hat{i}_q(k+1)L_q
\end{cases}
\tag{2}
$$

where R_s is the stator resistance; L_d, L_q are the stator inductance in the d-q axis; T_s is the sampling period; v_d, v_q are the stator voltages in the d-q axis; ω_r is the rotor electrical angular speed; ψ_d, ψ_q are the stator flux in the d-q axis; ψ_f is the permanent magnet flux.

The three-phase two level voltage source inverter (VSI) can generate 8 switching state combinations. The voltage vector corresponding to the switching state can be expressed as

$$
u_j = \frac{2}{3}V_{dc}(S_1 + aS_2 + a^2 S_3)
\tag{3}
$$

where $j = 0, \ldots., 7$ and $a = e^{i2\pi/3}$.

There are six active voltage vectors and two zero vectors, as shown in Figure 2.
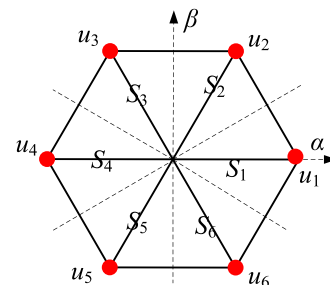

FIGURE 2. Space vector projection.

B. CONVENTIONAL MPC-FCS METHOD

The control scheme of the conventional FCS-MPC is illustrated in Figure 3. All the feasible voltage vectors in Figure 2 are enumerated and evaluated by a predefined cost function.
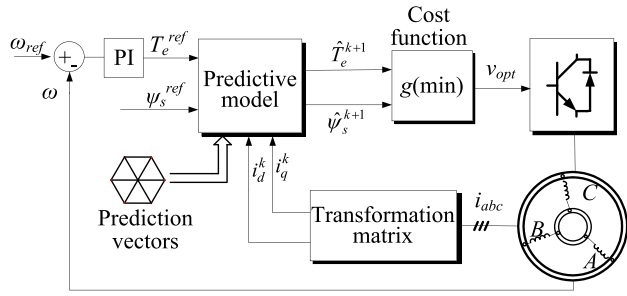
FIGURE 3. Control diagram of the conventional MPC method.

Generally, there are two forms of the cost function, which are

$$g_1 = \left| i_d^{ref} - \hat{i}_d(k+1) \right| + \left| i_q^{ref} - \hat{i}_q(k+1) \right| \quad (4)$$

$$g_2 = \left| T_e^{ref} - \hat{T}_e(k+1) \right| + \lambda \left| \psi_s^{ref} - \hat{\psi}_s(k+1) \right| \quad (5)$$

where T_e is the electromagnetic torque. The voltage vector that minimizes the cost function will be applied at next instant. Compared with the field-oriented control (FOC) and direct torque control (DTC), the FCS-MPC provides fast dynamic response and easy implementation. Unfortunately, the FCS-MPC requires a large amount of the time to enumerate all the feasible vectors. Besides, applying a single vector in each control period will result in large torque ripple. It can be explained by the fact that the optimal vector minimizes the cost function but the error can be further minimized if there are other candidates.

C. EXISTING REFERENCE VECTOR BASED MPC-FCS METHOD

To reduce the computational time, a natural option is to reduce the number of prediction vectors. In another word, the inappropriate voltage vectors should be excluded according to a certain constraint. A common practice is using the position of a reference vector, which have been widely investigated in [12], [13], [15], [16], [21]. The control scheme of the reference vector-based FCS-MPC is illustrated in Figure 4. The key is to directly derive a reference vector based on the deadbeat control principle. Subsequently, the useless vectors can be excluded according to the position of the
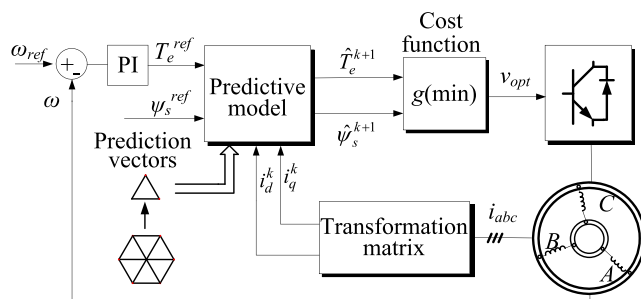
reference vector. In specific, the vectors that are closest to the reference vector will be selected as the prediction vectors.

Generally, there are two methods to determine the reference vector. One is using the deadbeat current control (DBCC) principle, where the stator currents at instant $k+1$ should be equal to the current command. The reference vector can be expressed as [16]

$$\begin{cases} v_d^{ref} = R_s \hat{i}_d(k+1) + \dfrac{L_d}{T_s}(i_d^{ref} - \hat{i}_d(k+1)) + e_d \\ v_q^{ref} = R_s \hat{i}_q(k+1) + \dfrac{L_q}{T_s}(i_q^{ref} - \hat{i}_q(k+1)) + e_q \end{cases} \quad (6)$$

Another alternative method to derive the reference vector is using the deadbeat torque and flux control (DTFC) [13], which is the intersection point of the torque line and the flux circle as shown in Figure 5. Unfortunately, both DBCC and DTFC involve intensive calculations to determine the reference vector. Generally, the sensitivity of DB-DTFC is mainly blamed on the flux linkage estimation rather than motor parameter estimation [22]. In addition, the sensitivity of DB-DTFC can be alleviated by employing advanced flux observers and stationary frame [22].
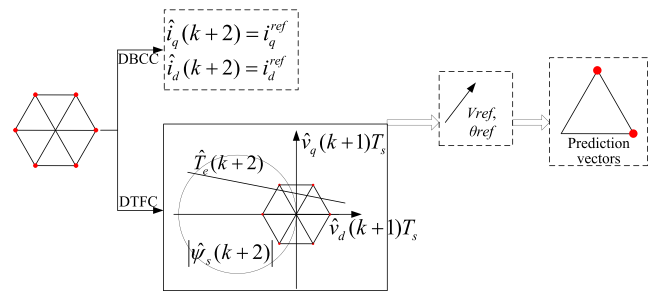

FIGURE 5. Prediction vector determination process based on reference vector.

III. PRINCIPLE OF THE PROPOSED METHOD
A. DISCRETE SPACE VECTOR MODULATION
To increase the robustness as well as avoid the complicated calculation, an indirect reference vector-based FCS-MPC method without using deadbeat control is presented in this section. The discrete space vector modulation (DSVM) technique is used to enhance the steady state performance. The control sets of voltage vectors can be extended by dividing the control period into several intervals. Assuming the control period is subdivided into N intervals, then the synthesized voltage for a two-level three-phase VSI can be expressed as

$$u^{syn} = \sum_{j=1,2,\dots,N} t_j u_j^{real} \quad (7)$$

where u_j^{real} is the actual vectors, $u_0, \dots u_7$, and

$$t_j = \frac{T_s}{N} \quad (8)$$

The total number of the feasible voltage vectors can be expressed as

$$n = 3N^2 + 3N + 2 \quad (9)$$

FIGURE 4. Control diagram of the MPC based on reference vector.

When $N = 2$, namely the control period is divided into two equal intervals, the total number of feasible vectors is 20, as shown in Figure 6. The red dots represent the actual vectors and the black and blue dots refer to the synthesized vectors. In specific, the black dots represent the vectors synthesized by two active vectors, for instance u_{12} is synthesized by u_1 and u_2. The blue dots are the vectors synthesized by one null vector and one active vector, for instance, u_{1Z} is synthesized by u_1 and a zero vector.
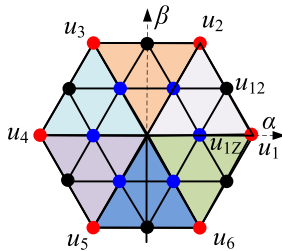

FIGURE 6. Discrete space vector projections.

B. VIRTUAL REFERENCE VECTOR DETERMINATION

Instead of directly calculating using deadbeat control, the reference vector is selected from six virtual vectors shown in Figure 7. The two-level hysteresis comparators-based DTC control theory is employed to determine the reference vector, except that the virtual vectors ($u_{12}, u_{23}, u_{34}, u_{45}, u_{56}, u_{61}$) are employed here instead of real vectors. The flux and torque are observed based on the following equations,

$$\psi_s = \int (u_s - R_s i_s) dt \tag{10}$$

$$T_e = \frac{3}{2} P_n (\psi_\alpha i_\beta - \psi_\beta i_\alpha) \tag{11}$$

where P_n is the number of pole pairs. Assume $\Delta\psi = \psi_{ref} - \psi_s$, $\Delta T_e = T_e^{ref} - T_e$, and $h_\psi = 1$ when $\Delta\psi > 0$, $h_\psi = 0$ when $\Delta\psi < 0$; $h_{Te} = 1$ when $\Delta T_e > 0$, $h_{Te} = 0$ when $\Delta T_e < 0$. Using this strategy, no intensive calculations are involved. It is worth to mention that the accuracy of the flux estimation in the low speed region can be affected by the stator resistance variation as well as the inverter non-linearities, such as dead time and voltage drop of switching
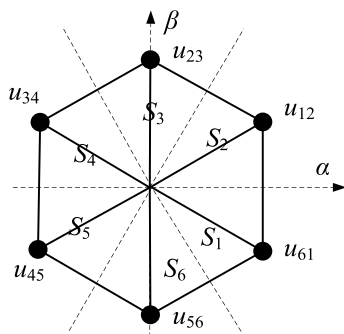
devices [23]. Many efforts have been made to deal with this problem [24]–[27]. An adaptive sliding observer is developed to estimate the flux based on current model in [24]. The effects of stator resistance variation and the voltage drop of power switches are compensated for the low speed operation in [25]. The reference vector selected at different conditions are summarized in Table 1, where S represents the sector the flux vector located.

TABLE 1. The look-up table based DTC for reference vector determination.

$h\psi$	h_{Te}	S					
		1	2	3	4	5	6
1	1	u_{12}	u_{23}	u_{34}	u_{45}	u_{56}	u_{61}
	0	u_{56}	u_{61}	u_{12}	u_{23}	u_{34}	u_{45}
0	1	u_{23}	u_{34}	u_{45}	u_{56}	u_{61}	u_{12}
	0	u_{45}	u_{56}	u_{61}	u_{12}	u_{23}	u_{34}

With the reference vector confirmed, the prediction vectors to be evaluated can be determined. The α-β plane is divided into 6 triangular regions, as shown in Figure 6. The vectors that locate in the same region with the reference vector are selected as the prediction vectors. For instance, if the reference vector is u_{12}, the prediction vectors will be u_{12}, u_1, u_2, u_{1Z}, u_{2Z} and a zero vector. Thus, the total number of prediction vectors is 6, which is even smaller than the conventional MPC for three-phase machine drives, where there are 7 vectors to be evaluated.

C. REAL REFERENCE VECTOR DETERMINATION

In section B, the reference vector is selected from the six virtual vectors $u_{12}, u_{23}, u_{34}, u_{45}, u_{56}, u_{61}$, and the number of prediction vectors is 6. Another alternative is selecting the reference vector from the six real vectors, $u_1, u_2, u_3, u_4, u_5, u_6$. Similarly, the DTC theory is employed to determine the reference vector. The look-up table is given in Table 2. In Figure 8, six rhomnic regions are formed to include each real vector. The vectors that locate in the same rhombic regions with the reference vector will be selected as the prediction vectors. For instance, if the reference vector determined using Table 2 is u_2, the prediction vectors will be $u_2, u_{12}, u_{2Z}, u_{23}$ and a zero vector. Thus, the total number will be 5, which is also smaller than 7.
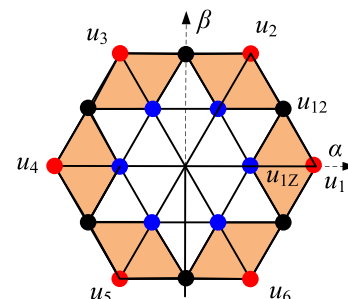

FIGURE 8. Rhombic regions defined in the α-β plane.

D. COST FUNCTION DESIGN

With the prediction vectors determined, the next step is to evaluate them with the cost function. Either cost function (4)
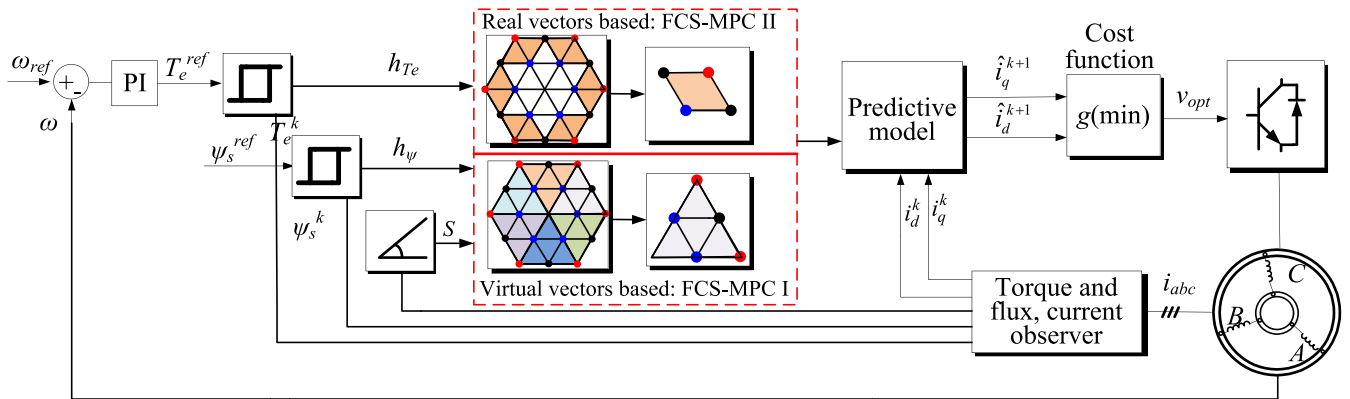

FIGURE 7. The reference vectors group.

FIGURE 9. The control scheme of the proposed method.

TABLE 2. The look-up table based DTC for reference vector determination.

$h\psi$	h_{Te}	S					
		1	2	3	4	5	6
1	1	u_2	u_3	u_4	u_5	u_6	u_1
	0	u_6	u_1	u_2	u_3	u_4	u_5
0	1	u_3	u_4	u_5	u_6	u_1	u_2
	0	u_5	u_6	u_1	u_2	u_3	u_4

or (5) can be used. To avoid the weighting factor tuning, the cost function (4) is adopted here. The two-step prediction introduced in [28] is also used to eliminate the error caused by time delay. The total number of feasible vectors is 20 if the control period is divided into two equal intervals. While using the proposed method, the number of prediction vectors is reduced to 5 or 6. Therefore, this method not only improves the control performance, but also reduces the computation time. Most importantly, the computation time is reduced without complicated reference vector derivation. It is worth to mention that the FCS-MPC is sensitive to the parameter variations since its predictive model highly depends on machine parameters. This problem can be alleviated by adopting disturbance observers to estimate the machine parameters [29], [30]. Meanwhile, the model free predictive control has also been presented to enhance the parameter robustness in [31], [32], where the knowledge of machine parameter is not required to predict the future behavior of the machine. The control scheme of the proposed method is illustrated in Figure 9. It is noted that the proposed method using the virtual vectors as reference vector (introduced in Section III-B) is termed as 'proposed FCS-MPC I'; and the method using the real vectors as reference vector (introduced in Section III-C) is termed as 'proposed FCS-MPC II'.

The overall control scheme of the proposed method is described as follows.

1) determine the reference vector using the two hysteresis comparators based DTC theory, as given in Table 1 OR Table 2.

2) Confirm the prediction vectors according to the selected reference vector, as shown in Figure 6 or Figure 8.

3) Evaluate the prediction vectors using the cost function (4).

4) Apply the optimal vector at the next instant.

IV. SIMULATION PERFORMANCES

In this section, the simulations are carried out in the environment of Matlab/Simulink to verify the effectiveness of the proposed method. The conventional model predictive current control (MPCC) method is also implemented as benchmark method. A 1.1 kW three-phase motor is used in the simulation. The parameters of the machine are listed in Table 3. The sampling frequency is set as 10 kHz for all methods in the simulation.

First, the steady state performance of the machine is investigated at 1500 rpm with full load for the conventional MPC method, the proposed FCS-MPC I and FCS-MPC II. It can be seen from Figure 10 that the phase current amplitude reaches 4 A at the full load condition. The current waveforms are sinusoidal for all methods. However, the current ripple of the conventional MPC method is slightly larger than the proposed methods. In addition, larger torque ripple is also presented in the conventional MPC method. This can be explained by the fact that the extended voltage vector sets in the proposed method can better track the current command.

Meanwhile, similar current and torque performance is presented by proposed FCS-MPC I and FCS-MPC II. This can be justified by the fact that the same vector will be selected though the reference vector determination process is different.

Secondly, the dynamic test is carried out to further evaluate these three methods. The machine accelerates from standstill to rated speed at instant 0.1s. The waveforms of the speed, torque and phase a current are shown in Figure 11. The zoomed plot of the torque is also added for better view of the torque ripple. It can be seen that the transient state for all methods are smooth. In another word, the proposed methods can achieve similar dynamic response speed with the
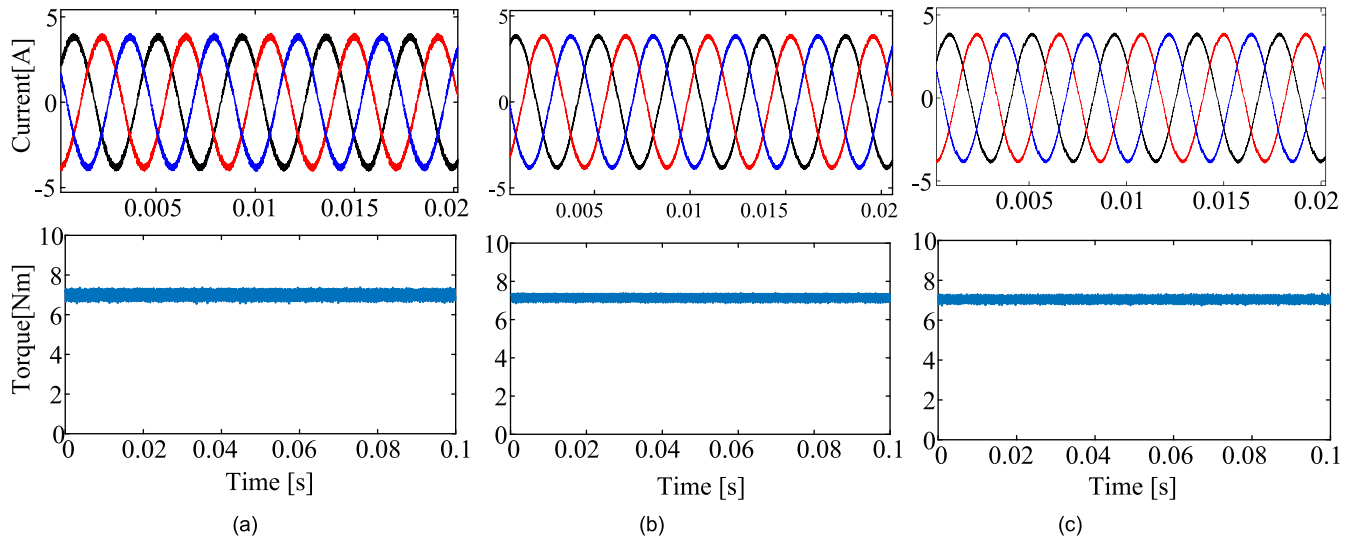
FIGURE 10. Steady state performance of the machine at 1500 rpm with full load. (a) conventional MPC method, (b) Proposed FCS-MPC I. (c) Proposed FCS-MPC II.
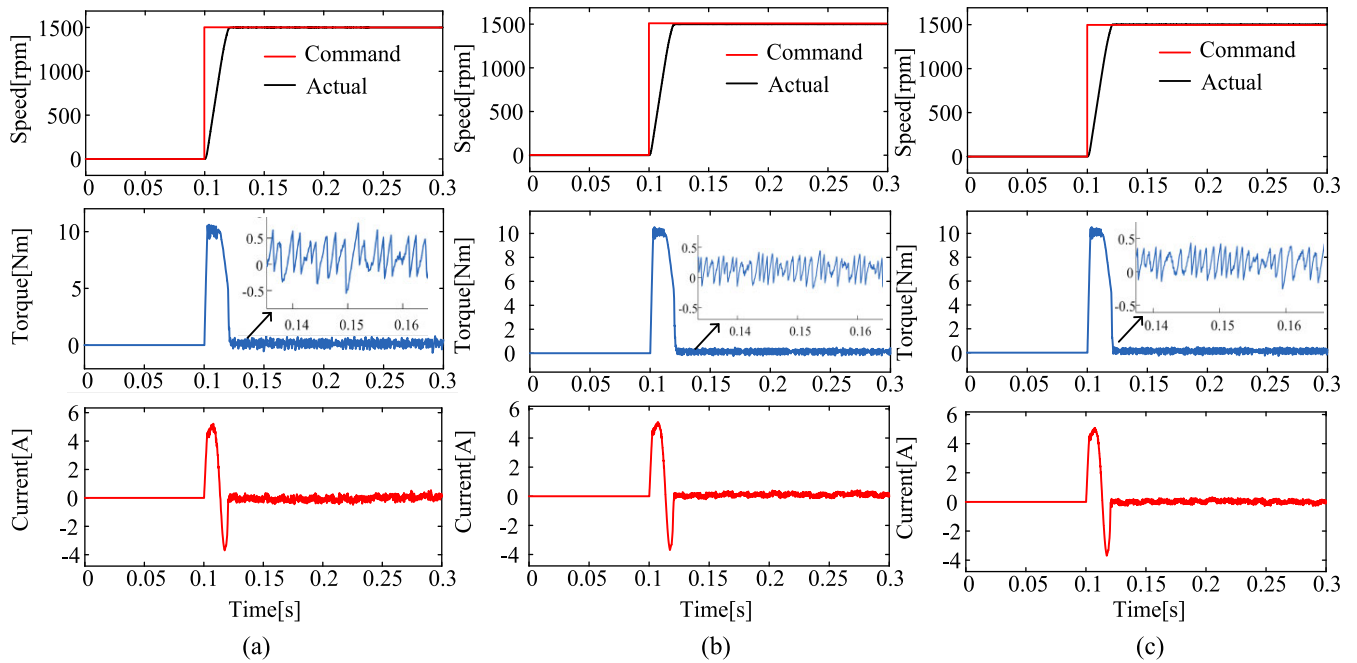

FIGURE 11. Dynamic performance of the machine. (a) conventional MPC method, (b) Proposed FCS-MPC I. (c) Proposed FCS-MPC II.

conventional MPC method but present better steady state performance. It is noted that the starting torque can be set as rated by limiting the output of speed controller in the simulation. However, in the practical situation, the starting torque usually exceeds the rated torque. Therefore, the starting torque is set around 10 Nm in the simulation, which is consistent with the practical value.

V. EXPERIMENTAL PERFORMANCES

The experimentations are conducted to prove the effectiveness of the proposed method in this section. A 1.1 kW three-phase PMSM motor based on the dSPACE 1103 is used. The experiment setup is illustrated in Figure 12. The conventional MPCC method for the three-phase PMSM motor is also conducted as the benchmark method. The sampling frequency is set as 10 kHz. The parameters of the machine and the control system are illustrated in Table 3. The value of the speed controller used is $k_p = 0.8$, $k_i = 0.35$ in the rate speed with full load. The cost function used in the proposed method is same as the conventional MPC, namely equation (4).

First, the steady-state performance of the machine running at rated speed with full load is investigated. The waveforms

TABLE 3. Key parameters of machine and control system.

Specification	Value
Rated motor power	1.1 kW
Rated speed	1500 rpm
Rated torque	7 Nm
Number of pole pairs	3
Stator resistance	4.5 Ω
d-axis inductance	0.012 H
q-axis inductance	0.014 H
Stator flux	0.21 Wb
Rotary inertia	0.0013 kg*m^2
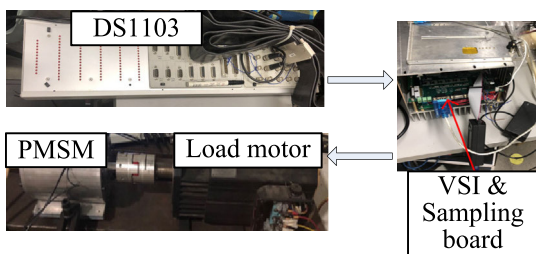
FIGURE 12. The experiment setup.

of the phase current, electromagnetic torque and speed are shown in Figure 13. It can be seen that the proposed method presents better current quality than the conventional MPC

method. The total harmonic distortion (THD) of the phase current shown in Figure 14 also demonstrate the superiority of the proposed method. In addition, it can be seen from Figure 13 that the torque ripple presented by the proposed method is also smaller than the conventional method. To be specific, the torque ripple of the proposed method is 0.32 Nm while that of the conventional method is 0.58 Nm. This can be explained by the fact that employing more prediction vectors by subdividing the control period into two equal intervals achieves better torque command tracking capability.

To further explore the superiority of the proposed method, the current THD are measured at different load conditions at rated speed for the conventional MPC, proposed FCS-MPC I, proposed FCS-MPC II and the conventional FOC method. It is seen from Figure 15 that the proposed method always present better current quality at different operating points than the conventional MPC. It can be seen that the FOC can present slightly lower THD than the proposed MPC method. This can be justified that the FOC can synthesize a desired vector using the SVPWM technique to track the command, rather than apply discrete vectors in the MPC method. However, as a different control technique, the MPC method possesses some advantages over the FOC, such as fast dynamic response, flexibility of including objective constraints [33], [34].

In addition, the torque ripple comparison at different speed conditions with rated load is given in Figure 16. It can be observed that the proposed method can achieve smaller torque ripple than the conventional MPC method. Meanwhile, the performance of the proposed FCS-MPC I, the
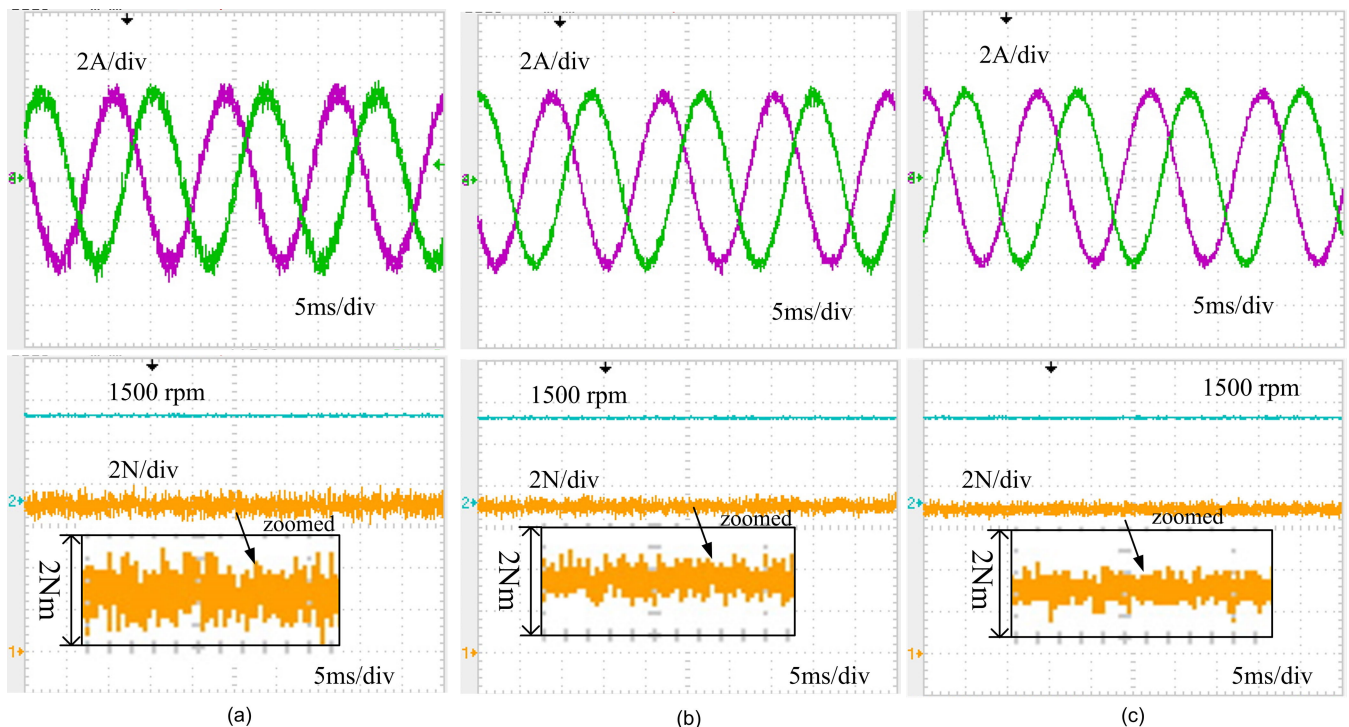

FIGURE 13. Steady-state performances of the machine at 1500 rpm with rate load. (a) conventional MPC method, (b) Proposed FCS-MPC I. (c) Proposed FCS-MPC II.

TABLE 4. Key parameters of machine and control system.

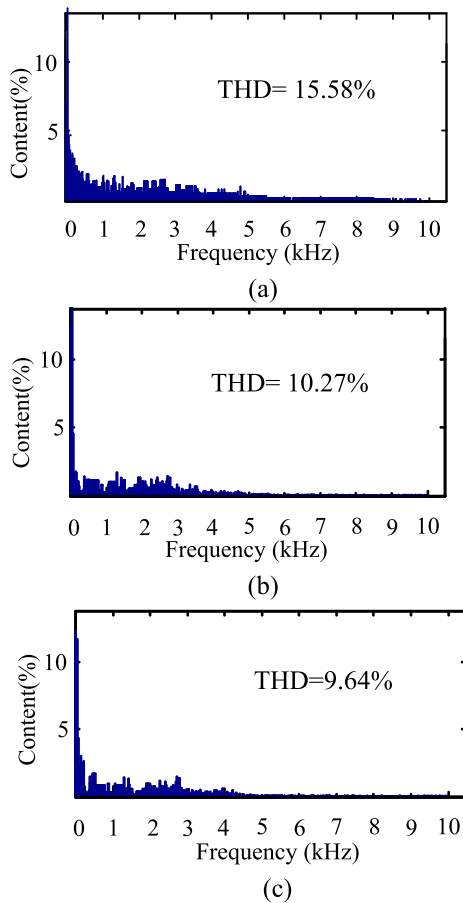| Control Method	Measurement (μs)	Reference vector determination (μs)	Prediction and evaluation (μs)	Total (μs)	Parameter sensitivity
Conventional MPC	7.32	0	48.51	55.83	High
Proposed FCS-MPC I	7.25	5.62	39.36	52.23	High
Proposed FCS-MPC II	7.31	5.45	37.43	50.19	High
DBCC based MPC	7.29	7.38	36.78	51.45	High
FOC	-	-	-	13.2	Low
DBCC	-	-	-	15.4	High
DB-DTFC	-	-	-	15.8	High

FIGURE 14. THD spectrum of phase currents. (a) conventional MPC method, (b) Proposed FCS-MPC I. (c) Proposed FCS-MPC II.

FIGURE 15. Stator current THD comparison among the conventional MPC, the proposed FCS-MPC I, and the proposed FCS-MPC II.

FIGURE 16. Torque ripple comparison among the conventional MPC, the proposed FCS-MPC I, and the proposed FCS-MPC II.

proposed FCS- MPC II are similar. The computation time for all methods are also measured in the steady state, as shown in Table 4. In addition, the total computation time of conventional FOC, DBCC and DTFC methods are also measured. It is seen that the MPC methods cost large computational time due to the enumeration process, compared with the FOC, DBCC and DB-DTFC methods. However, the computation time of the proposed method is slightly smaller than the conventional MPC. Thus, it is concluded that the proposed method can improve the control performance without requiring higher capability processors to implement the algorithm.
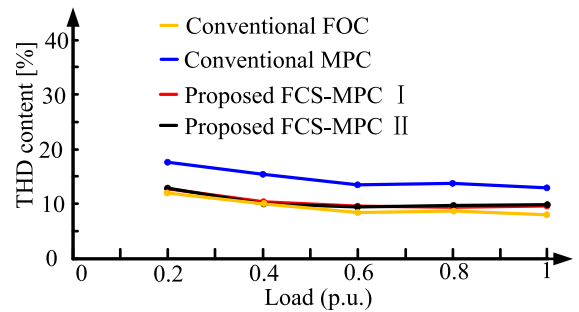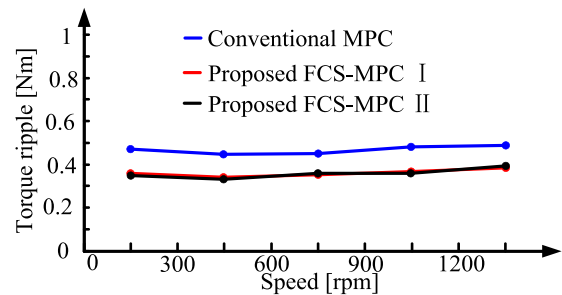
The conventional FCS-MPC, the proposed FCS-MPC and the DBCC based MPC all requires the knowledge of the motor parameters to predict future behavior, and the disturbance observers are not studied in this paper. Therefore, the conventional FCS-MPC, the proposed FCS-MPC and the DBCC based MPC are sensitive to the machine parameters, especially stator inductance and magnet flux [29]. The DBCC method also requires the stator resistance, inductance and magnet flux to calculate the current in next instant [35]. The mismatch of these parameters will cause prediction error. In addition, the parameter sensitivity problem of DB-DTFC mainly owes to the flux estimation [22]. The FOC method requires the knowledge of the rotor flux position to achieve decoupling of the torque- and flux-producing components [36]. However, the knowledge of the stator inductance and magnet flux magnitude is not required in the FOC method, which makes the FOC not as sensitive as
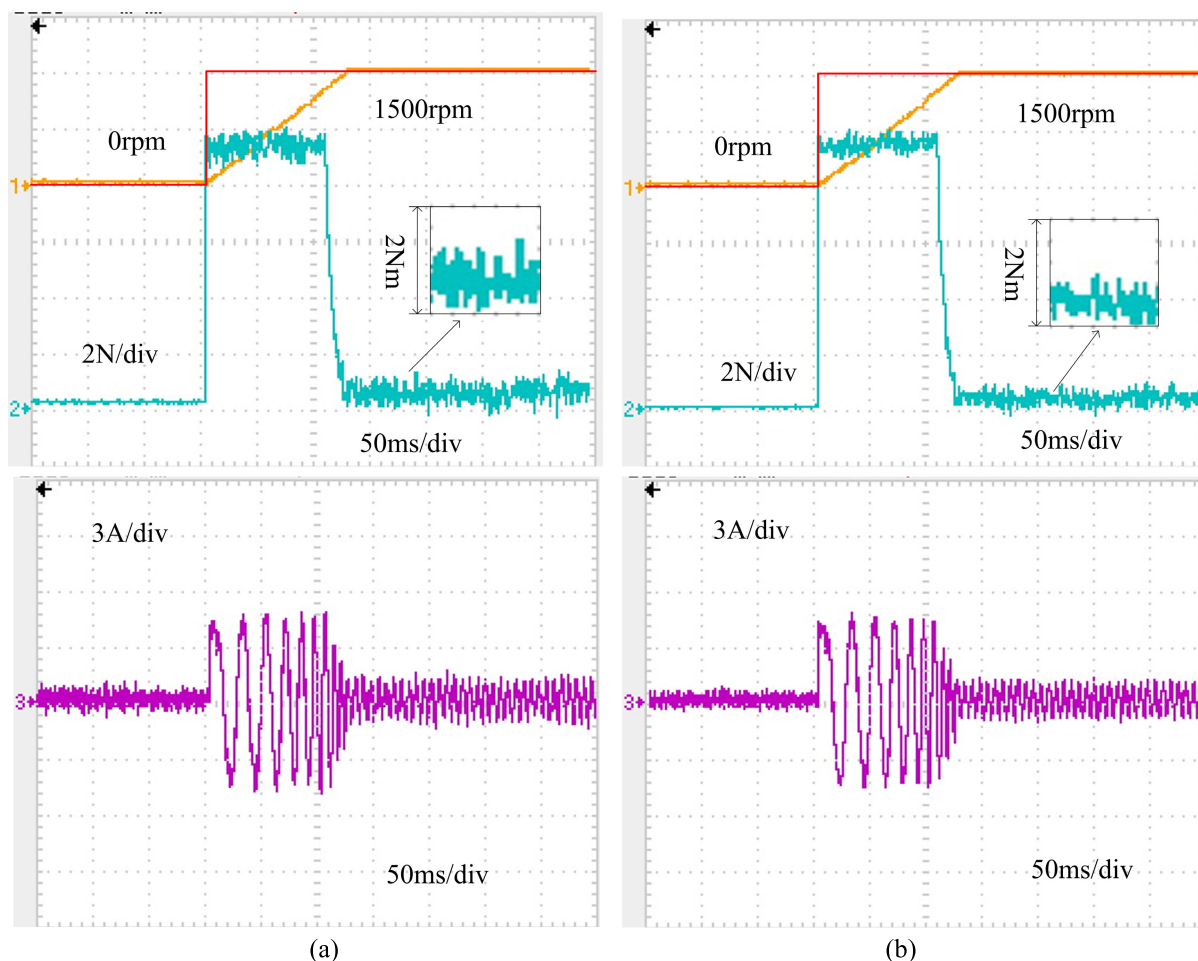
FIGURE 17. Dynamic performances of the machine accelerating from standstill to 1500 rpm without load. (a) proposed FCS-MPC I, (b) Proposed FCS-MPC II.

MPC or deadbeat control methods to machine parameter mismatch. To conclude, the MPC and deadbeat control methods listed in Table 4 are sensitive to machine parameters. While the robustness of FOC is stronger than the MPC and deadbeat control methods. Nevertheless, it is difficult to evaluate all the methods' robustness quantitatively. Therefore, the parameter sensitivity of all the methods are only compared qualitatively in Table 4.

Secondly, the dynamic performance of the proposed method is investigated when the machine is accelerating from standstill to rated speed. It can be seen from Figure 17 the transient waveform of the speed is smooth. The total acceleration process takes around 125ms, namely 1250 control periods. The torque and current performance are also given in Figure 17.

VI. CONCLUSION

This paper proposes an indirect reference vector based FCS-MPC method for a three-phase PMSM motor. The innovation point is that the reference vector is determined indirectly using the DTC theory instead of deadbeat control. In specific, two different strategies are presented according to the reference vector group. One is selecting the reference

vector from the virtual vectors and the other is selecting from the real vectors. Then the prediction vectors are determined according to the position of the reference vector. The number of prediction vectors is reduced from 20 to 6 and 5, respectively. Compared with deadbeat control based FCS-MPC, the intensive reference vector derivation is avoided. In addition, compared with the conventional MPC, the DSVM technique improves the control performance in terms of current THD and torque ripple, as indicated by the results. Meanwhile, the computation time is not sacrificed by extending the control sets of voltage vectors from 8 to 20, thanks to the proposed strategy. The simulation and experimental results are presented to verify the effectiveness of the proposed method.

REFERENCES

[1] A. Darba, F. De Belie, P. D'Haese, and J. A. Melkebeek, "Improved dynamic behavior in BLDC drives using model predictive speed and current control," *IEEE Trans. Ind. Electron.*, vol. 63, no. 2, pp. 728–740, Feb. 2016.

[2] J. Liu, C. Gong, Z. Han, and H. Yu, "IPMSM model predictive control in flux-weakening operation using an improved algorithm," *IEEE Trans. Ind. Electron.*, vol. 65, no. 12, pp. 9378–9387, Dec. 2018.

[3] W. Xie, X. Wang, F. Wang, W. Xu, R. Kennel, and D. Gerling, "Dynamic loss minimization of finite control set-model predictive torque control for electric drive system," *IEEE Trans. Power Electron.*, vol. 31, no. 1, pp. 849–860, Jan. 2016.

[4] M. Rivera, V. Yaramasu, A. Llor, J. Rodriguez, B. Wu, and M. Fadel, "Digital predictive current control of a three-phase four-leg inverter," *IEEE Trans. Ind. Electron.*, vol. 60, no. 11, pp. 4903–4912, Nov. 2013.

[5] F. Villarroel, J. R. Espinoza, C. A. Rojas, J. Rodriguez, M. Rivera, and D. Sbarbaro, "Multiobjective switching state selector for finite-states model predictive control based on fuzzy decision making in a matrix converter," *IEEE Trans. Ind. Electron.*, vol. 60, no. 2, pp. 589–599, Feb. 2013.

[6] Y. Zhang and H. Yang, "Model predictive torque control of induction motor drives with optimal duty cycle control," *IEEE Trans. Power Electron.*, vol. 29, no. 12, pp. 6593–6603, Dec. 2014.

[7] Y. Luo and C. Liu, "Multi-vector-based model predictive torque control for a six-phase PMSM motor with fixed switching frequency," *IEEE Trans. Energy Convers.*, vol. 34, no. 3, pp. 1369–1379, Sep. 2019, doi: 10.1109/tec.2019.2917616.

[8] L. Yan, M. Dou, Z. Hua, H. Zhang, and J. Yang, "Optimal duty cycle model predictive current control of high-altitude ventilator induction motor with extended minimum stator current operation," *IEEE Trans. Power Electron.*, vol. 33, no. 8, pp. 7240–7251, Aug. 2018.

[9] L. Yan, M. Dou, and Z. Hua, "Disturbance compensation-based model predictive flux control of SPMSM with optimal duty cycle," *IEEE J. Emerg. Sel. Topics Power Electron.*, vol. 7, no. 3, pp. 1872–1882, Sep. 2019, doi: 10.1109/jestpe.2018.2859979.

[10] Y. Luo and C. Liu, "Model predictive control for a six-phase PMSM with high robustness against weighting factor variation," *IEEE Trans. Ind. Appl.*, vol. 55, no. 3, pp. 2781–2791, May 2019.

[11] M. R. Nikzad, B. Asaei, and S. O. Ahmadi, "Discrete duty-cycle-control method for direct torque control of induction motor drives with model predictive solution," *IEEE Trans. Power Electron.*, vol. 33, no. 3, pp. 2317–2329, Mar. 2018.

[12] S. Vazquez, "Model predictive control with constant switching frequency using a discrete space vector modulation with virtual state vectors," in *Proc. IEEE Int. Conf. Ind. Technol.*, Feb. 2009, pp. 1–6, doi: 10/1109/ICIT.2009.4939728.

[13] Y. Wang, X. Wang, W. Xie, and F. Wang, "Deadbeat model-predictive torque control with discrete space-vector modulation for PMSM drives," *IEEE Trans. Ind. Electron.*, vol. 64, no. 5, pp. 3537–3547, May 2017.

[14] Y. Luo and C. Liu, "Elimination of harmonic currents using a reference voltage vector based-model predictive control for a six-phase PMSM motor," *IEEE Trans. Power Electron.*, vol. 34, no. 7, pp. 6960–6972, Jul. 2019.

[15] D. Casadei, G. Serra, and K. Tani, "Implementation of a direct control algorithm for induction motors based on discrete space vector modulation," *IEEE Trans. Power Electron.*, vol. 15, no. 4, pp. 769–777, 2000.

[16] J.-K. Kang and S.-K. Sul, "New direct torque control of induction motor for minimum torque ripple and constant switching frequency," *IEEE Trans. Ind. Appl.*, vol. 35, no. 5, pp. 1076–1082, 1999.

[17] Y. Zhang, D. Xu, and L. Huang, "Generalized multiple-vector-based model predictive control for PMSM drives," *IEEE Trans. Ind. Electron.*, vol. 65, no. 12, pp. 9356–9366, Dec. 2018.

[18] Y. Zhang, Y. Bai, and H. Yang, "A universal multiple-vector-based model predictive control of induction motor drives," *IEEE Trans. Power Electron.*, vol. 33, no. 8, pp. 6957–6969, Aug. 2018.

[19] Y. Luo and C. Liu, "A simplified model predictive control for a dual three-phase PMSM with reduced harmonic currents," *IEEE Trans. Ind. Electron.*, vol. 65, no. 11, pp. 9079–9089, Nov. 2018.

[20] M. Habibullah, D. D.-C. Lu, D. Xiao, and M. F. Rahman, "A simplified finite-state predictive direct torque control for induction motor drive," *IEEE Trans. Ind. Electron.*, vol. 63, no. 6, pp. 3964–3975, Jun. 2016.

[21] X. Zhang and B. Hou, "Double vectors model predictive torque control without weighting factor based on voltage tracking error," *IEEE Trans. Power Electron.*, vol. 33, no. 3, pp. 2368–2380, Mar. 2018.

[22] Y. Wang, Y. Shi, Y. Xu, and R. D. Lorenz, "A comparative overview of indirect field oriented control (IFOC) and deadbeat-direct torque and flux control (DB-DTFC) for AC motor drives," *Chin. J. Electr. Eng.*, vol. 1, no. 1, pp. 9–20, Dec. 2015.

[23] A. Yoo and S.-K. Sul, "Design of flux observer robust to interior permanent-magnet synchronous motor flux variation," *IEEE Trans. Ind. Appl.*, vol. 45, no. 5, pp. 1670–1677, 2009.

[24] Z. Xu and M. Rahman, "An adaptive sliding stator flux observer for a direct-torque-controlled IPM synchronous motor drive," *IEEE Trans. Ind. Electron.*, vol. 54, no. 5, pp. 2398–2406, Oct. 2007.

[25] L. Tang, F. Rahman, and M. Haque, "Low speed performance improvement of a direct torque controlled interior permanent magnet synchronous machine drive," in *Proc. 19th Annu. IEEE Appl. Power Electron. Conf. Exposit. (APEC)*, vol. 1, Jun. 2004, pp. 558–564.

[26] M. N. Uddin, H. Zou, and F. Azevedo, "Online loss-minimization-based adaptive flux observer for direct torque and flux control of PMSM drive," *IEEE Trans. Ind. Appl.*, vol. 52, no. 1, pp. 425–431, Jan. 2016.

[27] G. H. B. Foo and M. F. Rahman, "Direct torque control of an IPM-synchronous motor drive at very low speed using a sliding-mode stator flux observer," *IEEE Trans. Power Electron.*, vol. 25, no. 4, pp. 933–942, Apr. 2010.

[28] P. Cortes, J. Rodriguez, C. Silva, and A. Flores, "Delay compensation in model predictive current control of a three-phase inverter," *IEEE Trans. Ind. Electron.*, vol. 59, no. 2, pp. 1323–1325, Feb. 2012.

[29] X. Zhang, L. Zhang, and Y. Zhang, "Model predictive current control for PMSM drives with parameter robustness improvement," *IEEE Trans. Power Electron.*, vol. 34, no. 2, pp. 1645–1657, Feb. 2019.

[30] J. Wang, F. Wang, Z. Zhang, S. Li, and J. Rodriguez, "Design and implementation of disturbance compensation-based enhanced robust finite control set predictive torque control for induction motor systems," *IEEE Trans. Ind. Informat.*, vol. 13, no. 5, pp. 2645–2656, Oct. 2017.

[31] C.-K. Lin, J.-T. Yu, Y.-S. Lai, and H.-C. Yu, "Improved model-free predictive current control for synchronous reluctance motor drives," *IEEE Trans. Ind. Electron.*, vol. 63, no. 6, pp. 3942–3953, Jun. 2016.

[32] P. G. Carlet, F. Tinazzi, S. Bolognani, and M. Zigliotto, "An effective model-free predictive current control for synchronous reluctance motor drives," *IEEE Trans. Ind. Appl.*, vol. 55, no. 4, pp. 3781–3790, Jul. 2019.

[33] P. Cortés, M. P. Kazmierkowski, R. M. Kennel, D. E. Quevedo, and J. Rodríguez, "Predictive control in power electronics and drives," *IEEE Trans. Ind. Electron.*, vol. 55, no. 12, pp. 4312–4324, Dec. 2008.

[34] R. S. Dastjerdi, M. A. Abbasian, H. Saghafi, and M. H. Vafaie, "Performance improvement of permanent-magnet synchronous motor using a new deadbeat-direct current controller," *IEEE Trans. Power Electron.*, vol. 34, no. 4, pp. 3530–3543, Apr. 2019.

[35] X. Yuan, S. Zhang, and C. Zhang, "Enhanced robust deadbeat predictive current control for PMSM drives," *IEEE Access*, vol. 7, pp. 148218–148230, 2019.

[36] S. R. P. Reddy and U. Loganathan, "Robust and high-dynamic-performance control of induction motor drive using transient vector estimator," *IEEE Trans. Ind. Electron.*, vol. 66, no. 10, pp. 7529–7538, Oct. 2019.

SHUANGXIA NIU (Senior Member, IEEE) received the B.Sc. and M.Sc. degrees in electrical engineering from the School of Electrical Engineering and Automation, Tianjin University, Tianjin, China, and the Ph.D. degree in electrical engineering from The University of Hong Kong, Hong Kong, in 2009.

Since 2009, she has been with The Hong Kong Polytechnic University, Hong Kong, where she is currently an Associate Professor with the Department of Electrical Engineering. She has authored or coauthored more than 100 articles in leading journals. Her research interests include the design and control of novel electrical machines and drives, renewable energy conversion systems, and applied electromagnetics.

YIXIAO LUO (Student Member, IEEE) was born in Hubei, China, in 1991. He received the B.Eng. degree from Wuhan University, Wuhan, China, in 2013, the M.Eng. degree from Hanyang University, South Korea, in 2015, and the Ph.D. degree from the City University of Hong Kong, in 2019, all in electrical engineering.

He is currently a Research Associate with The Hong Kong Polytechnic University. His research interests include motor drives and power electronics.

WEINONG FU received the B.Eng. degree from the Hefei University of Technology, Hefei, China, in 1982, the M.Eng. degree from the Shanghai University of Technology, Shanghai, China, in 1989, and the Ph.D. degree from The Hong Kong Polytechnic University, Hong Kong, in 1999, all in electrical engineering. He is currently a Professor with The Hong Kong Polytechnic University. Before joining the university in 2007, he was one of the Key Developers at Ansoft Corporation, Pittsburgh, PA, USA. He has about seven years of working experience at Ansoft, focusing on the development of the commercial software Maxwell. His current research interests include electromagnetic field computation, applied electromagnetics, and novel electric machines.

XIAODONG ZHANG (Student Member, IEEE) received the B.Eng. and M.Eng. degrees from Tianjin University, Tianjin, China, in 2002 and 2005, respectively, and the Ph.D. degree in electrical engineering from The University of Hong Kong, Hong Kong, in 2011. His research interests include electric machine design, motor control, renewable energy conversion, switching-mode power supplies, and hybrid electric vehicles.

• • •